Hindawi
Advances in Materials Science and Engineering
Volume 2022, Article ID 3973469, 11 pages
https://doi.org/10.1155/2022/3973469

Research Article

Research on Shield Tunnelling Parameters Correlation in Composite Strata

Ziqi Guo,[1] Huipeng Zhang,[2] Xiaoyang Shi,[1] Zhi Huang,[1] Yiyong Xu,[1] and Zhiqiang Zhang[3]

[1]*China Railway No. 5 Engineering Group Co. Ltd., 410007 Changsha, China*
[2]*Nanchang Urban Rail Group Co. Ltd., 330038 Nanchang, China*
[3]*School of Civil Engineering, Southwest Jiaotong University, 610031 Chengdu, China*

Correspondence should be addressed to Zhiqiang Zhang; clarkchang68@163.com

Received 24 January 2022; Revised 2 March 2022; Accepted 21 March 2022; Published 1 April 2022

Academic Editor: Yonghong Wang

Shield tunnelling has become the development direction of tunnel construction due to its safety, economy, and speed. The complex formation has complicated geological changes, including soft rock, hard rock, and soft and hard inhomogeneous formation. It is particularly difficult to select and control the tunnelling parameters in shield tunnelling, while the reasonable selection and control of the tunnelling parameters play an important role in the excavation efficiency, tool wear, and surface settlement. Based on the tunnel project between the Dinggong Road North Station and the People's Park Station online 4 of Nanchang Metro during shield tunnelling construction, this paper collects thrust, torque, and revolution speed of the cutterhead during shield tunnelling in the complex strata with differentiated argillaceous siltstone and gravel and analyzes these parameters by means of mathematical statistics analysis, in order to explore the interrelationship between shield tunnelling parameters under different stratigraphic conditions and put forward optimization suggestions for tunnelling parameters, which can provide a reference for control of tunnelling parameters of earth pressure shield in composite strata.

1. Introduction

With a rapid increase in the construction of underground structures, shield tunnelling has been widely used in China's metro construction [1–5]. To ensure the stability of the excavation surface and to control ground settlement, the earth pressure balance (EPB) shield must be reasonably matched to the construction parameters during excavation [6–8]. Shield tunnelling operation affects project scheduling, cost estimation, and safety risk during metro construction [9, 10]. Tunnelling by the shield method in a single stratum is relatively easy, with relatively single and stable tunnelling parameters and mode and relatively simple construction technology [11, 12]. However, the application of the shield method for urban subway tunnels in composite strata with uneven hardness and frequent changes in rock properties is faced with many challenges [13], such as the adaptability of the shield [14], the reasonable selection of tunnelling parameters [15], and the control of the impact on the surrounding environment during the tunnelling process [16, 17].

The shield tunnelling process is a socio-technical complex system with high uncertainty and nonlinear phenomena in temporal evolution [18]. Specifically, the main parameters for shield tunnelling include cutterhead rotation speed, cutterhead torque, screw machine rotation speed, screw machine torque, shield thrust, and shield advance rate [19]. At present, many researchers use qualitative or quantitative approaches to analyze the tunnelling parameters of TBMs [20–22]. Farrokh and Rostami [23] studied the correlation of tunnel convergence with TBM operational parameters and chip size and found that tunnel convergence has shown a strong relationship with the TBM thrust/torque and rate of penetration (ROP). Armaghani et al. [24] developed several optimization techniques for predicting the advanced rate of tunnel boring machines (TBMs) in different weathered zones of granite. Liu et al. [25] proposed an intelligent decision method for the main control parameters of tunnel boring machines based on multiobjective optimization of excavation efficiency and cost. Aiming at the problem that it is difficult to accurately predict and correct the axis attitude deviation in the shield tunnelling process, Wang et al. [26] put forward a prediction of axis attitude deviation and a deviation correction method based on data driven during shield tunnelling. Wei et al. [27] studied the prediction of TBM driving speed based on the BP neural network model of the machine learning method. Xu et al. [28] analyzed the relationships between the TBM operating parameters and daily collected TBM data. Zhou et al. [29] addressed the characteristics of shield tunnelling parameters (total thrust, torque, penetration rate, rotation rate, advance speed, and working chamber pressure) by introducing a visibility graph model implemented in a complex network of shield tunnelling in metro construction.

At present, there are mainly theoretical calculation methods and empirical prediction methods for the prediction of shield tunnelling speed and cutterhead torque. In terms of theoretical calculations, based on a large number of statistical data, the CSM model developed by the Colorado School of Mines [30, 31] was proposed to predict parameters such as cutterhead torque and tunnelling speed. Wang and Fu [32] established the geometric continuity equation, physical equation, and balance equation for shield tunnelling, and combined with the regression analysis of shield construction parameters records, the relationships among each tunnelling parameter were verified. For empirical prediction, Barton [33] introduced tunnelling parameters based on the rock quality index Q to form the Q_{TBM} model for the prediction of the tunnelling speed. Bruland [34] used the shield construction parameters database as the basis, combined with indoor tests such as rock brittleness tests and wear tests, to establish the NTNU model to predict the tunnelling parameters such as the tunnelling speed. In the theoretical calculation model, the accuracy of prediction results is determined by the selection of key parameters, which need to be obtained from specific tests and have limitations in engineering applications in complex formations. The Q_{TBM} model has too many parameters, which affects its engineering application. The NTNU model is not applicable to hard but poorly integrated formations.

The geological conditions in Nanchang are very complex, and the shield excavation section shows a typical composite stratum, which is manifested by a wide range of geological changes in the excavation direction and the unevenness of the surrounding rock in the excavation section. In order to improve the prediction accuracy of tunnelling parameters in complex strata, this paper takes the tunnel project of Dinggong Road North Station, People's Park Station of Nanchang Metro Line 4 constructed by shield tunnelling as its support and carries out geological segmentation and sectional statistical tunnelling parameters for complex strata based on the basic quality index of equivalent rock mass in the full section of palm face. In this paper, a large number of tunnelling parameters of typical composite strata are combined with the analysis of tunnelling parameters by mathematical statistics and curve fitting methods, and the interrelationship between tunnelling parameters in different strata is derived. The conclusions and formulas obtained have direct engineering applicability and practical guiding significance for shield tunnelling in the later medium-differentiated argillaceous siltstone and gravel sand composite strata. At the same time, this method of mathematical and statistical analysis based on a large amount of data and combined with the analysis of construction data can provide a reference for the analysis of tunnelling parameters for shield construction in other composite strata. The empirical relational expressions obtained from the statistics of the field tunnelling data have important guiding significance for the parameter selection and matching in the design of the earth pressure balance shield.

2. Research Background

The interval between the Dinggong Road North Station and People's Park Station of Nanchang Rail Transit Line 4 is excavated by the shield method, with a total length of about 944 m. The tunnel support structure is a prefabricated reinforced concrete pipe sheet with a concrete strength grade of C50, its inner diameter is 5.4 m, outer diameter is 6 m, thickness is 0.3 m, and width is 1.5 m. The tunnel crosses mainly gravelly sand and medium-differentiated muddy siltstone strata and locally crosses upper-soft and lower-hard strata. The geological longitudinal section is shown in Figure 1. The geological conditions revealed by the drill holes are shown in Figure 2. The physical and mechanical parameters of the main geotechnical bodies are shown in Table 1. The types of groundwater at the site are divided into pore diving in the strongly weathered zone, fracture water in the strongly to moderately weathered bedrock, and upper layer stagnant water locally distributed in the artificial fill and clayey soil. Groundwater is encountered in all boreholes of the site. The water level in each borehole is measured from 3.20 to 9.80 m, and the depth of stable water level is 2.80 to 9.60 m. The change of groundwater level is closely related to the storage, recharge, and discharge of groundwater. After September, the water level decreases slowly as the precipitation decreases and is at a low water level from December to February of the following year.

3. Correlation Analysis of Shield Tunnelling Parameters in Different Stratigraphic Conditions

The tunnel between the Dinggong Road North Station and People's Park Station of Nanchang Metro Line 4 has typical full section soft strata (gravelly sand layer), upper-soft and lower-hard strata (gravelly sand and medium-differentiated mud siltstone composite strata), and full section harder rock strata (medium differentiated mud siltstone strata). The interrelationship between tunnelling parameters such as thrust, torque, revolution speed of the cutterhead, penetration, tunnelling speed, and chamber earth pressure varies for shield tunnelling construction in

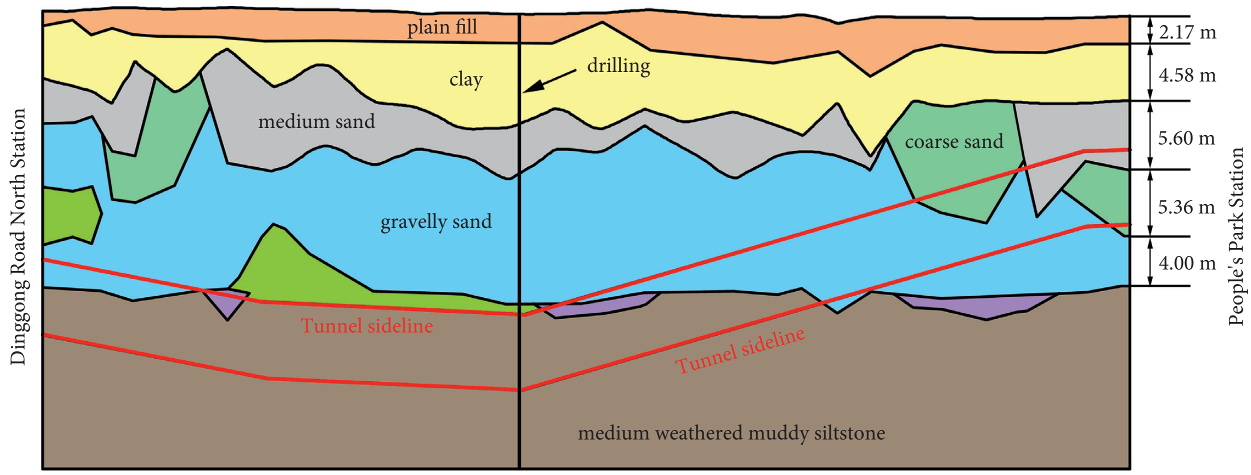

Figure 1: Schematic diagram of stratigraphic distribution.

(a) (b)

Figure 2: Geological conditions revealed by the drill holes.

different strata. According to the actual measurement data at the tunnel boring construction site, this paper analyzed the interrelationship of each tunnelling parameter in soft and weak strata, s upper-soft and lower-hard strata, and hard rock stratum in full section, respectively, and compared and analyzed the relationships between the tunnelling parameters of different strata in order to explore the relationship law of each tunnelling parameter under different strata.

Based on a strict mathematical and physical deduction basis and a semi-empirical approach, Wang and Fu [32] deduced the relationship between earth pressure balance shield, total thrust, screw conveyor speed, and tunnelling speed as shown in the following equations:

$$p\frac{\pi D^2}{4}\left[1+\frac{\delta}{p}[1-\lambda]\right] = P_0 + K\Delta S - K\left(\frac{4k_e\eta k\Delta S}{\gamma_0\pi D^2}\right)\frac{N}{v}, \quad (1)$$

$$T = (F + P_0 + K\Delta S) - K\left(\frac{4k_e\eta k\Delta S}{\gamma_0\pi D^2}\right)\frac{N}{v}, \quad (2)$$

where D is the diameter of shield machine; δ is the additional value of panel pressure; λ is the shield opening rate; P_0 is the static Earth pressure at the palm surface; K is the value of reaction force when the soil is deformed under contact pressure, which is called plausible stiffness; K_e is the effective Earth exit ratio; k is the parameter related to the form of screw conveyor; η is selected according to the surrounding rock and the efficiency of soil discharge; ΔS is the advancing

Table 1: Physical and mechanical parameters of rock and soil mass.

Geotechnical layer	Density (g/cm^3)	Natural water content (%)	Specific gravity	Porosity ratio	Direct fast shear test		Modulus of deformation (MPa)	Permeability coefficient (m/d)	Thermal conductivity (w/m·k)	Coefficient of rock or soil foundation (MPa/m)		Stratigraphic resistance factor (MN/m^3)	Poisson's ratio	Rock quality designation, RQD (%)
					Cohesion (kPa)	Angle of internal friction (°)				Horizontal	Vertical			
Vegetative fill	1.84	26.2	2.73	0.871	12	10	—	5	—	15	10	5	—	—
Clay	1.93	26.00	2.74	0.787	30	12	18	0.004	1.97	33	30	11	0.36	—
Medium sand	1.97	—	2.64	—	1	31	29	40	2.28	26	24	14	0.30	—
Coarse sand	1.98	—	2.64	—	1	34	32	80	2.23	30	26	16	0.29	—
Gravelly sand	2.00	—	2.63	—	1	36	33	100	2.06	35	30	20	0.29	—
Strongly weathered muddy siltstone	2.02	—	—	—	40	25	80	0.8	1.60	100	100	40	0.32	—
Medium-weathered muddy siltstone	2.25	—	—	—	350	32	—	0.1	2.06	220	220	60	0.27	40–90

distance; γ_0 is the natural heaviness of the soil; and F is the total resistance of the shield advancing.

According to the data recorded at the tunnel boring construction site of this project, by curve fitting the scatter diagrams of each tunnelling parameter of the earth pressure balance shield under soft and weak strata in full section, upper-soft and lower-hard composite strata, and a full section of harder rock strata, the corresponding relationship curve and relationship equation can be derived.

R^2 used in the curve fitting process is the goodness of fit, which measures the overall fit of the regression equation and expresses the overall relationship between the dependent variable and all independent variables. The value of R^2 is from 0 to 1. The closer the value of R^2 is to 1, the better the fit of the regression line to the observed values; conversely, the smaller the value of R^2 is, the worse the fit of the regression line to the observed values. In this study, the number of statistical samples of tunnelling parameters is large and there are many construction influencing factors. Therefore, we can consider $R^2 = 0\sim0.09$ as no correlation, $R^2 = 0.0\sim0.2$ as weak correlation, $R^2 = 0.2\sim0.5$ as medium correlation and $R^2 = 0.5\sim1.0$ as strong correlation.

3.1. *Analysis of the Relationship Law of Tunnelling Parameters in Full-Section Soft Strata*

3.1.1. Interrelationship of Chamber Earth Pressure with Revolution Speed of Screw Conveyor and Tunnelling Speed. The revolution speed of the screw conveyor is mainly controlled manually and does not change much, and the revolution speed of screw conveyor in this section is 1 r/min~3 r/min. Since the depth of the selected shield interval does not change much, it can be considered that P_0 is approximately constant. According to equation (1), it can be found that the chamber earth pressure is approximately proportional and negatively correlated with the ratio of screw conveyor revolution speed to tunnelling speed. Based on the measured data recorded at the construction site of the shield tunnelling in the relying interval, the scatter diagram of the chamber Earth pressure vs the ratio of screw conveyor speed to tunnelling speed is drawn as shown in Figure 3. From the figure, it can be concluded that the chamber earth pressure is approximately proportional to the ratio of screw conveyor revolution speed to tunnelling speed when the shield is tunnelling in a full section of soft ground, where $R^2 = 0.6747$, indicating a strong correlation. The slope is −179.154, indicating a negative correlation, which is consistent with the prediction. Through statistical regression analysis, the relationship between the chamber earth pressure and the ratio of screw conveyor revolution speed to tunnelling speed in the full section of soft ground is derived as shown in following equation:

$$p = \frac{-179.154N}{v + 5.961}. \quad (3)$$

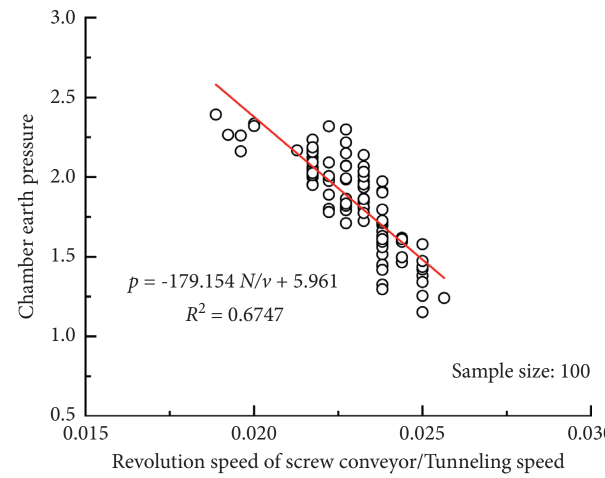

Figure 3: N/v vs. p curve in full section soft strata.

3.1.2. Interrelationship of Total Thrust with the Revolution Speed of Screw Conveyor and the Tunnelling Speed. Since the depth of burial of the selected shield interval does not vary much, it can be assumed that $(F + P_0 + K\Delta S)$ is approximately constant. According to equation (2), the total thrust is approximately proportional and negatively correlated with the ratio of screw conveyor revolution speed to tunnelling speed. Based on the measured data recorded at the tunnelling construction site, the scatter plot of the total thrust vs the ratio of screw conveyor speed to tunnelling speed is drawn as shown in Figure 4.

From the figure, it can be seen that when the shield is dug in a full section of soft ground, the total thrust is approximately proportional to the ratio of screw conveyor speed to tunnelling speed, where $R^2 = 0.3899$, which is moderately correlated. It is due to the fact that the F term has many influencing factors and keeps changing during the digging process, treating it as a constant term will cause the data in the figure to deviate. The slope is −68991.125 and it is negative correlation, which is consistent with the prediction. Through statistical regression analysis, the relationship between the total thrust and the ratio of screw conveyor revolution speed to the tunnelling speed of the soft strata in the full section is derived as shown in following equation

$$T = \frac{-68991.125N}{v + 2659.397}. \quad (4)$$

3.1.3. Interrelationship of Cutterhead Torque with Total Thrust, Revolution Speed of Cutterhead, and Earth Pressure. The above analysis does not consider two important tunnelling parameters: the revolution speed of the cutterhead and cutterhead torque. It is still difficult to derive the relationship between the cutterhead torque and the revolution speed of the cutterhead based entirely on the mathematical physical model. Therefore, a semi- empirical method is adopted to derive them. According to many projects, it is known that there is a certain linear relationship between the cutterhead torque and the total thrust. Figure 5 shows the scatter plot of the measured cutterhead torque and total

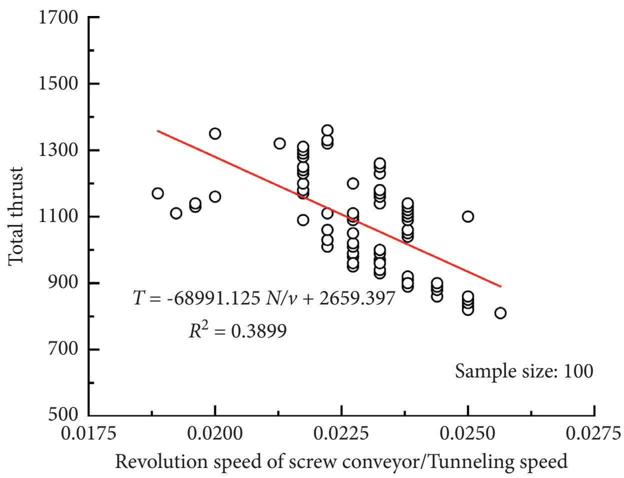

Figure 4: N/v vs. T curve in full section soft strata.

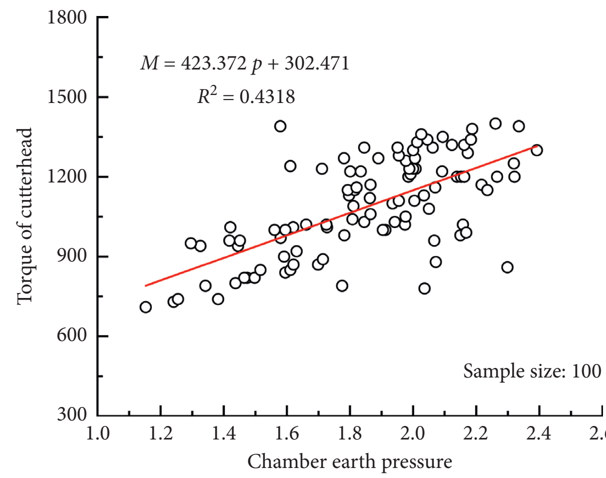

Figure 6: p vs. M curve in full-section soft strata.

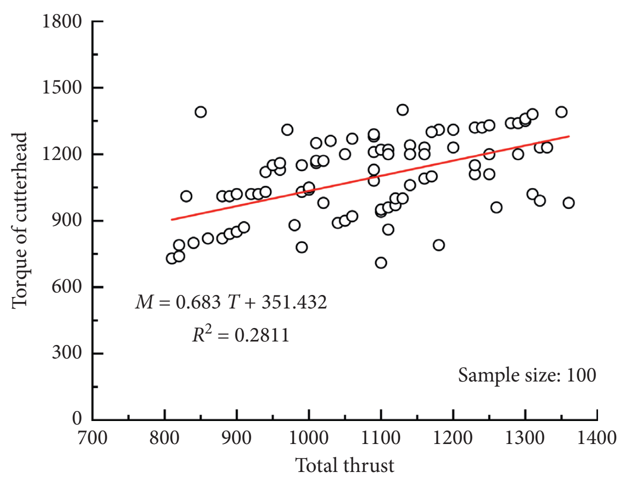

Figure 5: T vs. M curve in full-section soft strata.

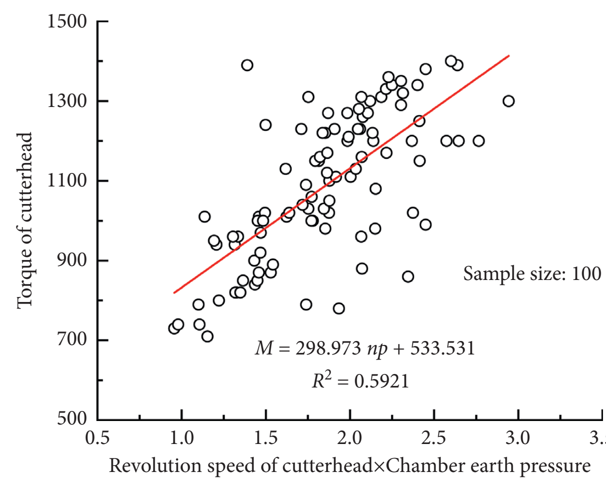

Figure 7: $n{\cdot}p$ vs. M curve in full section soft strata.

thrust data in the field. From the figure, it can be seen a moderate correlation, $R^2 = 0.2811$, when shield tunnelling in soft strata. Through statistical regression analysis, the relationship between the cutterhead torque and total thrust for a full section of soft strata is derived as shown in the following equation:

$$M = 0.683T + 351.432. \tag{5}$$

According to the theoretical analysis of Wang and Fu [32], it can be assumed that the chamber earth pressure has a direct effect on the magnitude of the cutterhead torque. The scatter plot of the field measured chamber earth pressure and cutterhead torque data is shown in Figure 6. From the figure, it can be seen that there is a moderate correlation between the cutterhead torque and chamber earth pressure when tunnelling under soft strata, which is stronger than the correlation between the total thrust and the cutterhead torque mentioned above. Through statistical regression analysis, the relationship between the cutterhead torque and chamber earth pressure for a full section of soft strata is derived as shown in following equation:

$$M = 423.372p + 302.471. \tag{6}$$

The faster the revolution speed of the cutterhead, the higher the torque required. Figure 7 shows the scatter plot of (chamber earth pressure × revolution speed of cutterhead) vs. cutterhead torque data. From the figure, it can be seen that there is a strong correlation between $n{\cdot}p$ and M with $R^2 = 0.5921$ when the shield is tunnelled under the soft strata. Through statistical regression analysis, the relationship between the cutterhead torque and (chamber earth pressure × revolution speed of cutterhead) in soft strata is derived as shown in the following equation::

$$M = 298.973np + 533.531. \tag{7}$$

3.2. Analysis of the Relationship Law of Tunnelling Parameter in the Upper-Soft and Lower-Hard Strata. At present, research on the control of tunnelling parameters in the upper-soft and lower-hard strata is still at a weak stage, while the control of tunnelling parameters in the upper-soft and lower-hard composite strata is the key to tunnel construction. In this section, based on the data recorded at the construction site of interval tunnelling, the scatter diagram between each main tunnelling parameter is fitted by curves when the shield is tunnelled in the upper-soft and lower-hard strata. The corresponding relationship curves and relationship equations are derived, and the correlation is evaluated using the decision coefficient R^2.

3.2.1. Correlation between the Cutterhead Torque and the Revolution Speed of Cutterhead. When tunnelling in the upper-soft and lower-hard strata, the cutterhead torque is generally larger due to the complex geological conditions and difficulty of tunnelling. In order to control the shield machine power, the revolution speed of cutterhead should be reduced accordingly, when the cutterhead torque is larger. Figure 8 shows the scatter plot of the cutterhead torque vs the revolution speed of the cutterhead. From the figure, it can be seen that there is a medium correlation between the revolution speed of cutterhead and the cutterhead torque when the shield tunnelling in the upper-soft and lower-hard strata. The revolution speed of cutterhead tends to increase first and then decrease with the increase of the cutterhead torque. According to the equation of the fitted curve, when the cutterhead torque is less than 1250 kN·m, the revolution speed of cutterhead increases slowly with the cutterhead torque; when the cutterhead torque is greater than 1250 kN·m, the revolution speed of cutterhead shows a decreasing trend with the increase of the cutterhead torque. This is due to the fact that in the upper-soft and lower-hard strata, the cutterhead torque is generally larger, sometimes even reaching its shield rated torque value, and the revolution speed of the cutterhead needs to be reduced in order to control the power of shield tunnelling. From the perspective of controlling cutter deflection wear, the revolution speed of the cutterhead should also be reduced. Through statistical regression analysis, the relationship between the revolution speed of the cutterhead and the cutterhead torque is shown in equation (8) when shield tunnelling in the upper-soft and lower-hard strata.

$$n = -1.100M^2 + 3.051M + 1.374. \quad (8)$$

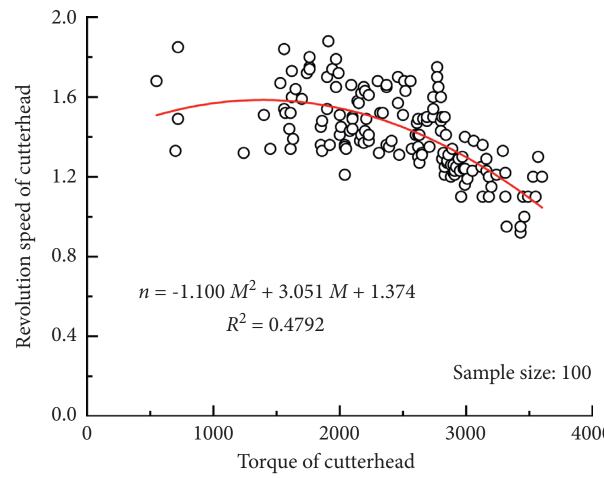

Figure 8: M vs. n curve in upper-soft and lower-hard strata.

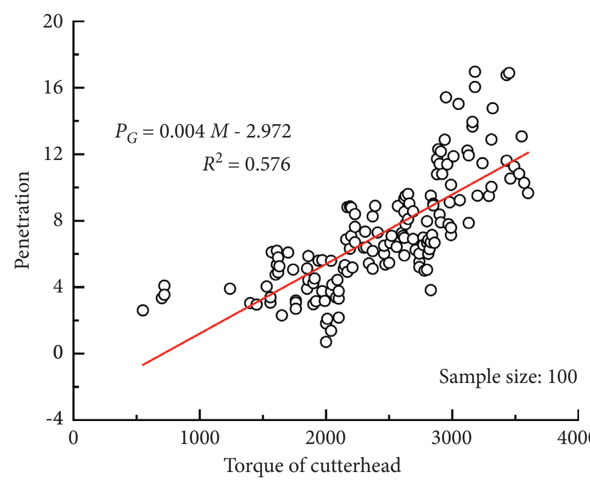

Figure 9: M vs. P_G curve in upper-soft and lower-hard strata.

3.2.2. The Correlation of the Cutterhead Torque with Total Thrust and Penetration. For the same surrounding rock, increasing penetration inevitably increases torque, which means that the torque increases with increasing penetration in the same surrounding rock conditions. In addition, there is an inherent relationship between the total thrust and the cutterhead torque. Based on the data recorded in the field when the shield tunnelling in the upper-soft and lower-hard strata of the inter district tunnel project, the scatter diagrams of the cutterhead torque vs penetration and total thrust are drawn as shown in Figures 9 and 10, respectively.

From the figure, it can be seen that the coefficient of determination R^2 between penetration and the cutterhead torque is 0.579, and the coefficient of determination R^2 between total thrust and the cutterhead torque is 0.555 when shield tunnelling in the upper-soft and lower-hard strata, both of which show a moderate correlation. This is because the relationship between the cutterhead torque, the total thrust, and penetration is mainly influenced by human control due to the complex geology of the upper-soft and lower-hard strata. The difficulty in tunnelling and many other factors need to be considered. Through statistical regression analysis, the relationship between the cutterhead torque and penetration is shown in equation (9). The relationship between the cutterhead torque and total thrust when shield tunnelling in the upper-soft and lower-hard strata is shown in the following equation:

$$P_G = 0.004M - 2.972, \quad (9)$$

$$T = 0.313M + 1981.871. \quad (10)$$

3.2.3. The Interrelationship between Penetration and Total Thrust. The penetration and the total thrust are the two main parameters of the excavation construction. The penetration and the total thrust are intrinsically related, and the magnitude of

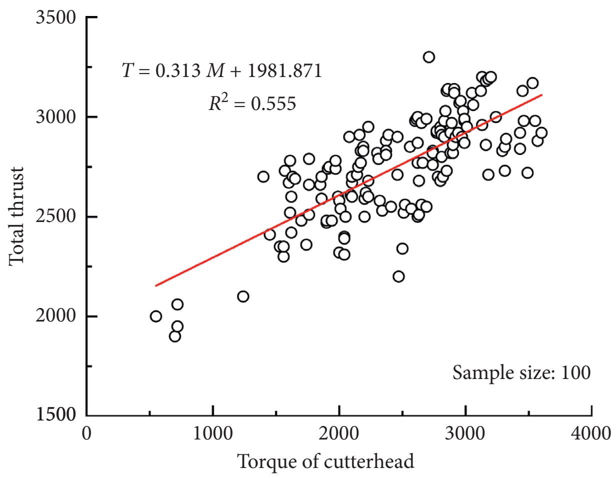

Figure 10: M vs. P_G curve in upper-soft and lower-hard strata.

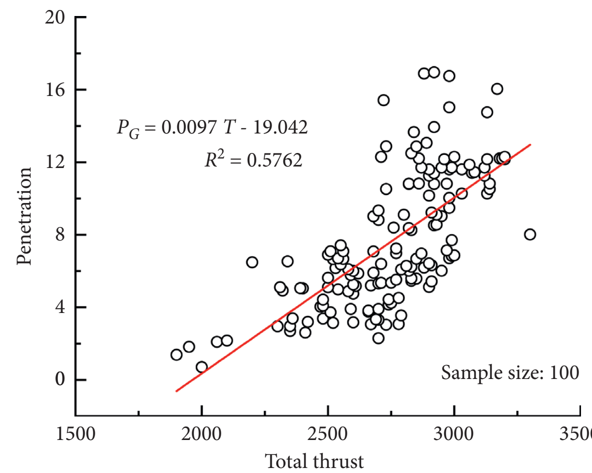

Figure 11: T vs. P_G curve in upper-soft and lower-hard strata.

the penetration is determined by the magnitude of the total thrust. In general, the higher the total thrust, the higher the penetration. Based on the measured penetration and total thrust data recorded at the tunnel site, the total thrust vs. penetration scatter diagram is drawn, as shown in Figure 11. From the figure, it can be seen that there is a positive correlation between the penetration and the total thrust when shield tunnelling in the upper-soft and lower-hard strata and $R^2 = 0.5762$, which is a strong correlation. The penetration increases with the increase of the total thrust. Through statistical regression analysis, the relationship between the penetration and the total thrust for tunnelling in the upper-soft and lower-hard strata is shown in the following equation:

$$P_G = 0.0097T - 19.042. \tag{11}$$

3.2.4. The Interrelationship between Chamber Earth Pressure and Total Thrust. The chamber earth pressure is related to the balance of the palm surface and is one of the key parameters for surface settlement control. Based on the measured chamber earth pressure and total thrust data recorded at the tunnel site, the scatter diagram of the chamber earth pressure and total thrust is drawn, as shown in Figure 12. From the figure, it can be seen that there is no correlation between the chamber earth pressure and the total thrust at when tunnelling in the upper-soft and lower-hard strata. This is because the geology is complicated in the upper-soft and lower-hard strata. In such circumstances, the excavation is difficult and the surface settlement is not easily controlled. In order to strictly control the surface settlement, the chamber earth pressure needs to be controlled in a relatively high range. The matching relationship between the chamber earth pressure and the total thrust is mainly influenced by human control, which is reflected as the human control variable relationship. Through statistical regression analysis, the relationship between the chamber earth pressure and total thrust during excavation in the upper-soft and lower-hard strata is shown in the following equation:

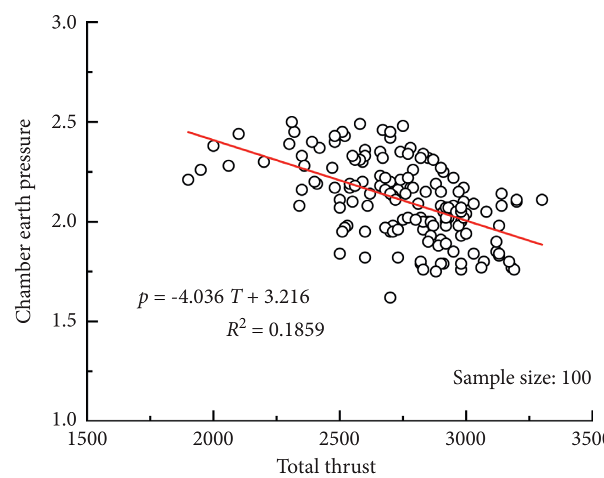

Figure 12: T vs. p curve in upper-soft and lower-hard strata.

$$p = -4.036T + 3.216. \tag{12}$$

3.3. Analysis of the Relationship Law between Each Tunnelling Parameter in Full-Section Hard Rock Strata. In this section, based on the data recorded at the construction site of the interval tunnel, the relationship between penetration, total thrust, cutterhead torque, revolution speed of the cutterhead, and tunnelling speed is studied. The relationship between each major tunnelling parameter when the shield is tunnelled through a full section of hard rock strata is fitted by curves, and the corresponding relationship curves and relationship equations are derived. The R^2 is used to evaluate the correlation.

3.3.1. The Correlation of Penetration with Total Thrust and Cutterhead Torque. The penetration is an important index of cutter breaking. In general, the penetration is directly related to the total thrust and the cutterhead torque, and the penetration can be controlled by adjusting the total thrust and the cutterhead torque. According to the data recorded at the tunnel boring construction site, the scatter plots of

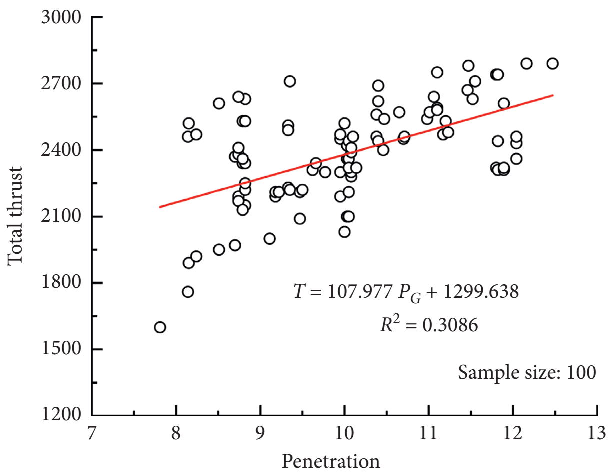

FIGURE 13: P_G vs. T curve in full section of harder rock strata.

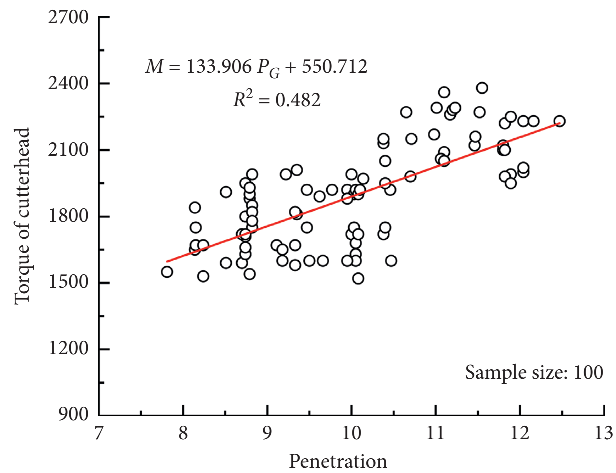

FIGURE 14: P_G vs. M curve in full section of harder rock strata.

penetration vs total thrust and cutterhead torque are shown in Figures 13 and 14. From the graphs, it can be concluded that there is a positive correlation between the total thrust and the penetration when shield tunnelling in full-section hard rock strata. And $R^2 = 0.3086$, which shows a medium correlation. The total thrust increases with the increase of penetration. There is a positive correlation between the cutterhead torque and penetration. And $R^2 = 0.482$, which shows a moderate correlation. The cutterhead torque increases with the increase of penetration. Through statistical regression analysis, the relationship between the penetration and total thrust when shield tunnelling in hard rock strata is shown in equation (13). The relationship between penetration and cutterhead torque is shown in equation (14):

$$T = 107.977P_G + 1299.638, \quad (13)$$

$$M = 133.906P_G + 550.712. \quad (14)$$

3.3.2. The Interrelationship of Revolution Speed of Cutterhead with Cutterhead Torque and Total Thrust. The revolution speed of the cutterhead is related to the efficiency of tunnelling. There is a direct relationship between the revolution speed of the cutterhead and cutterhead torque, which is also intrinsically related to the total thrust. According to the data recorded at the tunnel excavation site, the scatter diagrams of the revolution speed of the cutterhead vs cutterhead torque and total thrust are drawn, as shown in Figures 15 and 16. From the figure, it can be seen that there is a negative correlation between the cutterhead torque and the revolution speed of cutterhead. And $R^2 = 0.3568$, which shows a medium correlation. As the cutter speed increases, the cutterhead torque demand is decreasing. There is a negative correlation between total thrust and revolution speed of cutterhead. And $R^2 = 0.5680$, which shows a strong correlation. As the revolution speed of the cutterhead increases, the total thrust demand is decreasing. Through statistical regression analysis, the relationship between the revolution speed and cutterhead torque is derived as shown in equation

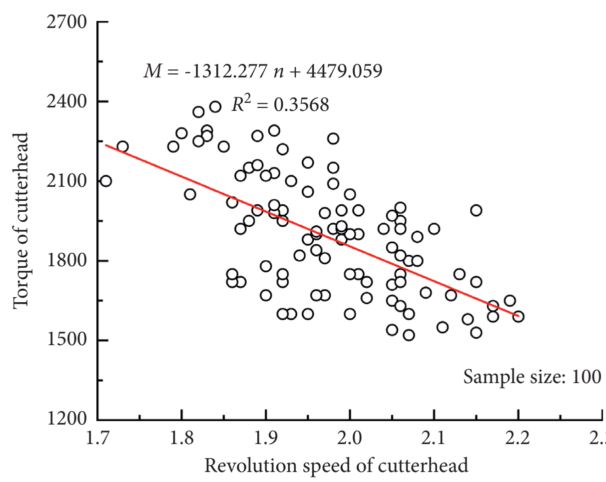

FIGURE 15: n vs M curve in full section of harder rock strata.

(15). The relationship between the revolution speed and total thrust of the cutterhead is derived as shown in equation (16):

$$M = -1312.277n + 4479.059, \quad (15)$$

$$T = -1667.931n + 5671.077. \quad (16)$$

3.3.3. The Interrelationship of Tunnelling Speed with Total Thrust and Cutterhead Torque. The tunnelling speed is an intuitive indicator of the efficiency of shield tunnelling construction, and the tunnelling speed is mainly controlled by the total thrust and cutterhead torque. Based on the data recorded at the tunnel excavation site, the scatter diagrams of tunnelling speed vs. cutterhead torque and total thrust are drawn, as shown in Figures 17 and 18, respectively. From the figure, it can be seen that there is a positive correlation between total thrust and tunnelling speed when shield tunnelling in hard rock strata. And $R^2 = 0.8321$, which shows a strong correlation. As the tunnelling speed increases, the total thrust demand also increases. There is a positive correlation between the torque of

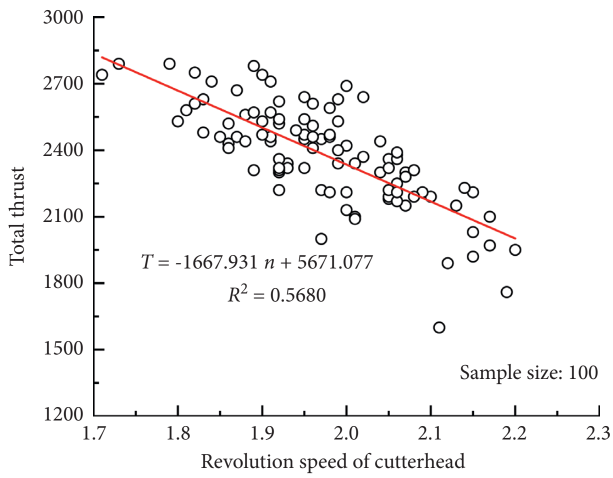

FIGURE 16: n vs T curve in full section of harder rock strata.

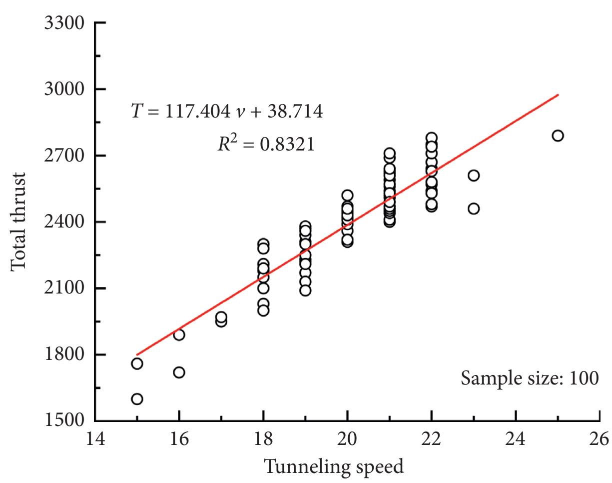

FIGURE 17: v vs. T curve in full section of harder rock strata.

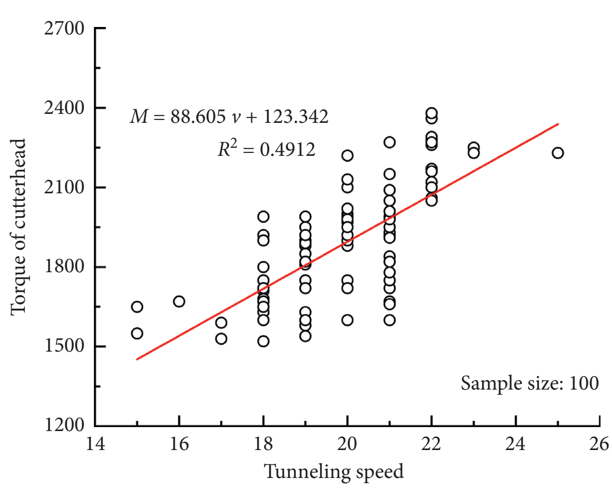

FIGURE 18: v vs. M curve in full section of harder rock strata.

the cuttterhead and the tunnelling speed. And $R^2 = 0.4912$, which shows a medium correlation. As the tunnelling speed increases, the cutterhead torque also increases.

$$\begin{aligned} T &= 117.404v + 38.714, \\ M &= 88.605v + 123.342. \end{aligned} \tag{17}$$

4. Conclusion

In the shield construction of composite strata, the selection of tunnelling parameters is closely related to the tunnelling efficiency and tunnelling safety. This paper investigates the laws of tunnelling parameters such as shield tunnelling speed, thrust, and torque, as well as the intrinsic relationship between each tunnelling parameter to provide reference for the control of shield construction parameters in composite strata. The following conclusions are drawn:

(1) The relationship between the cutterhead torque, the total thrust, and penetration is mainly influenced by human control due to the complex geology of the upper-soft and lower-hard strata. The difficulty in tunnelling and many other factors need to be considered.

(2) In order to strictly control the surface settlement in the upper-soft and lower-hard strata, the chamber earth pressure needs to be controlled in a relatively high range. The matching relationship between the chamber earth pressure and the total thrust is mainly influenced by human control.

(3) Through the mathematical and statistical analysis of a large number of similar projects, more accurate and widely applicable tunnelling parameter control standards, and control methods based on actual engineering experience can be derived.

Data Availability

The data used to support the findings of this study are available from the corresponding author upon request.

Conflicts of Interest

The authors declare that there are no conflicts of interest regarding the publication of this paper.

Acknowledgments

This research was supported by the funding from the General Program of National Natural Science Foundation of China (51878572) and the Science and Technology Program of Nanchang Urban Rail Group Co., Ltd. of China (2019HGKYB003).

References

[1] S. Guo, H. Luo, and L. Yong, "A big data-based workers behavior observation in China metro construction," *Procedia Engineering*, vol. 123, pp. 190–197, 2015.

[2] Q. Z. Yu, L. Y. Ding, C. Zhou, and H. B. Luo, "Analysis of factors influencing safety management for metro construction in China," *Accident Analysis & Prevention*, vol. 68, pp. 131–138, 2014.

[3] L. Ding, L. Zhang, X. Wu, M. J. Skibniewski, and Y. Qunzhou, "Safety management in tunnel construction: case study of Wuhan metro construction in China," *Safety Science*, vol. 62, pp. 8–15, 2014.

[4] D. Lin, J. D. Nelson, M. Beecroft, and J. Cui, "An overview of recent developments in China's metro systems," *Tunnelling and Underground Space Technology*, vol. 111, Article ID 103783, 2021.

[5] M. Li, H. Yu, H. Jin, and P. Liu, "Methodologies of safety risk control for China's metro construction based on BIM," *Safety Science*, vol. 110, pp. 418–426, 2018.

[6] X. Liu, S. Xu, and Y. Huang, "Optimal control for earth pressure balance of shield machine based on action-dependent heuristic dynamic programming," *ISA Transactions*, vol. 94, pp. 28–35, 2019.

[7] S. Mokhtari, W. Navidi, and M. Mooney, "White-box regression (elastic net) modeling of earth pressure balance shield machine advance rate," *Automation in Construction*, vol. 115, Article ID 103208, 2020.

[8] C. Shao and D. Lan, "Optimal control of an earth pressure balance shield with tunnel face stability," *Automation in Construction*, vol. 46, pp. 22–29, 2014.

[9] R. Wang, D. Li, E. J. Chen, and Y. Liu, "Dynamic prediction of mechanized shield tunneling performance," *Automation in Construction*, vol. 132, Article ID 103958, 2021.

[10] H. W. Huang, Y. J. Zhang, D. M. Zhang, and B. M. Ayyub, "Field data-based probabilistic assessment on degradation of deformational performance for shield tunnel in soft clay," *Tunnelling and Underground Space Technology*, vol. 67, pp. 107–119, 2017.

[11] S. S. Lin, S. L. Shen, N. Zhang, and A. Zhou, "Modelling the performance of EPB shield tunnelling using machine and deep learning algorithms," *Geoscience Frontiers*, vol. 12, Article ID 101177, 2021.

[12] W. Zhou, W. Nie, X. Liu et al., "Optimization of dust removal performance of ventilation system in tunnel constructed using shield tunneling machine," *Building and Environment*, vol. 173, Article ID 106745, 2020.

[13] S. Ma, Z. Duan, Z. Huang, Y. Liu, and Y. Shao, "Study on the stability of shield tunnel face in clay and clay-gravel stratum through large-scale physical model tests with transparent soil," *Tunnelling and Underground Space Technology*, vol. 119, Article ID 104199, 2022.

[14] G. Xu, C. He, D. Lu, and S. Wang, "The influence of longitudinal crack on mechanical behavior of shield tunnel lining in soft-hard composite strata," *Thin-Walled Structures*, vol. 144, Article ID 106282, 2019.

[15] X. Li, H. Di, S. Zhou, P. Huo, and Q. Huang, "Effective method for adjusting the uplifting of shield machine tunneling in upper-soft lower-hard strata," *Tunnelling and Underground Space Technology*, vol. 115, Article ID 104040, 2021.

[16] H. Xie, X. Duan, H. Yang, and Z. Liu, "Automatic trajectory tracking control of shield tunneling machine under complex stratum working condition," *Tunnelling and Underground Space Technology*, vol. 32, pp. 87–97, 2012.

[17] H. Luo, L. Li, and K. Chen, "Parametric modeling for detailed typesetting and deviation correction in shield tunneling construction," *Automation in Construction*, vol. 134, Article ID 104052, 2022.

[18] C. Zhou, L. Y. Ding, and R. He, "PSO-based Elman neural network model for predictive control of air chamber pressure in slurry shield tunneling under Yangtze River," *Automation in Construction*, vol. 36, pp. 208–217, 2013.

[19] T. Yan, S. L. Shen, A. Zhou, and H. M. Lyu, "Data on performance and variation index for shield tunnelling through soft deposit," *Data in Brief*, vol. 36, Article ID 107103, 2021.

[20] Y. D. Xue, F. Zhao, H. X. Zhao, X. Li, and Z. X. Diao, "A new method for selecting hard rock TBM tunnelling parameters using optimum energy: a case study," *Tunnelling and Underground Space Technology*, vol. 78, pp. 64–75, 2018.

[21] S. Heydari, J. H. Khademi, M. Monjezi, and A. Eftekhari, "An investigation of the relationship between muck geometry, TBM performance, and operational parameters: a case study in Golab II water transfer tunnel," *Tunnelling and Underground Space Technology*, vol. 88, pp. 73–86, 2019.

[22] X. Rong, H. Lu, M. Wang, and X. Rong, "Cutter wear evaluation from operational parameters in EPB tunneling of Chengdu Metro," *Tunnelling and Underground Space Technology*, vol. 93, Article ID 103043, 2019.

[23] E. Farrokh and J. Rostami, "Correlation of tunnel convergence with TBM operational parameters and chip size in the Ghomroud tunnel, Iran," *Tunnelling and Underground Space Technology*, vol. 23, no. 6, pp. 700–710, 2008.

[24] D. J. Armaghani, M. Koopialipoor, A. Marto, and S. Yagiz, "Application of several optimization techniques for estimating TBM advance rate in granitic rocks," *Journal of Rock Mechanics and Geotechnical Engineering*, vol. 11, no. 4, pp. 779–789, 2019.

[25] B. Liu, Y. Wang, G. Zhao et al., "Intelligent decision method for main control parameters of tunnel boring machine based on multi-objective optimization of excavation efficiency and cost," *Tunnelling and Underground Space Technology*, vol. 116, Article ID 104054, 2021.

[26] P. Wang, X. Kong, Z. Guo, and L. Hu, "Prediction of axis attitude deviation and deviation correction method based on data driven during shield tunneling," *IEEE Access*, vol. 7, pp. 163487–163501, 2019.

[27] M. Wei, Z. Wang, X. Wang, J. Peng, and Y. Song, "Prediction of TBM penetration rate based on Monte Carlo-bp neural network," *Neural Computing & Applications*, vol. 33, no. 2, pp. 603–611, 2021.

[28] C. Xu, X. Liu, E. Wang, and S. Wang, "Prediction of tunnel boring machine operating parameters using various machine learning algorithms," *Tunnelling and Underground Space Technology*, vol. 109, Article ID 103699, 2021.

[29] C. Zhou, L. Ding, Y. Zhou, and M. J. Skibniewski, "Visibility graph analysis on time series of shield tunneling parameters based on complex network theory," *Tunnelling and Underground Space Technology*, vol. 89, pp. 10–24, 2019.

[30] J. Rostami and L. Ozdemir, "New model for performance production of hard rock TBMs," in *Proceedings of the 1993 Rapid Excavation and Tunneling Conference*, Publ by Soc of Mining Engineers of AIME, Boston, Massachusetts, USA, June 1993.

[31] J. Rostami, *Development Of A Force Estimation Model For Rock Fragmentation With Disc Cutters Through Theoretical Modeling And Physical Measurement Of Crushed Zone Pressure*, Colorado School of Mines, Golden, Colorado, USA, 1997.

[32] H. Wang and D. Fu, "A mathematical model and the related parameters for EPB shield tunneling," *China Civil Engineering Journal*, vol. 9, pp. 86–90, 2006, (in Chinese).

[33] N. Barton, "TBM performance estimation in rock using Q(TBM)," *Tunnels and Tunnelling International*, vol. 31, pp. 30–34, 1999.

[34] A. Bruland, *Hard rock tunnel boring*, Ph.D. thesis, Norwegian university of Science and Technology, Trondheim, Norway, 1998.